Neuroscience 139 (2006) 639–649

PHOTOBIOMODULATION PARTIALLY RESCUES VISUAL CORTICAL NEURONS FROM CYANIDE-INDUCED APOPTOSIS

H. L. LIANG,[a] H. T. WHELAN,[b] J. T. EELLS,[c] H. MENG,[a] E. BUCHMANN,[b] A. LERCH-GAGGL[a] AND M. WONG-RILEY[a]*

[a]*Department of Cell Biology, Neurobiology and Anatomy, Medical College of Wisconsin, 8701 Watertown Plank Road, Milwaukee, WI 53226, USA*

[b]*Department of Neurology, Medical College of Wisconsin, 8701 Watertown Plank Road, Milwaukee, WI 53226, USA*

[c]*College of Health Sciences, University of Wisconsin–Milwaukee, Milwaukee, WI 53201, USA*

Abstract—Near-infrared light via light-emitting diode treatment has documented therapeutic effects on neurons functionally inactivated by tetrodotoxin or methanol intoxication. Light-emitting diode pretreatment also reduced potassium cyanide-induced cell death, but the mode of death via the apoptotic or necrotic pathway was unclear. The current study tested our hypothesis that light-emitting diode rescues neurons from apoptotic cell death. Primary neuronal cultures from postnatal rat visual cortex were pretreated with light-emitting diode for 10 min at a total energy density of 30 J/cm^2 before exposing to potassium cyanide for 28 h. With 100 or 300 μM potassium cyanide, neurons died mainly via the apoptotic pathway, as confirmed by electron microscopy, Hoechst 33258, single-stranded DNA, Bax, and active caspase-3. In the presence of caspase inhibitor I, the percentage of apoptotic cells in 300 μM potassium cyanide was significantly decreased. Light-emitting diode pretreatment reduced apoptosis from 36% to 17.9% (100 μM potassium cyanide) and from 58.9% to 39.6% (300 μM potassium cyanide), representing a 50.3% and 32.8% reduction, respectively. Light-emitting diode pretreatment significantly decreased the expression of caspase-3 elicited by potassium cyanide. It also reversed the potassium cyanide-induced increased expression of Bax and decreased expression of Bcl-2 to control levels. Moreover, light-emitting diode decreased the intensity of 5-(and -6) chloromethy-2′, 7-dichlorodihydrofluorescein diacetate acetyl ester, a marker of reactive oxygen species, in neurons exposed to 300 μM potassium cyanide. These results indicate that light-emitting diode pretreatment partially protects neurons against cyanide-induced caspase-mediated apoptosis, most likely by decreasing reactive oxygen species production, down-regulating pro-apoptotic proteins and activating anti-apoptotic proteins, as well as increasing energy metabolism in neurons as reported previously. © 2006 Published by Elsevier Ltd on behalf of IBRO.

*Corresponding author. Tel: +1-414-456-8467; fax: +1-414-456-6517.
E-mail address: mwr@mcw.edu (M. Wong-Riley).

Abbreviations: CM-H_2DCFDA, 5-(and -6) chloromethy-2′, 7-dichlorodihydrofluorescein diacetate acetyl ester; DAB, 3,3′-diaminobenzidine; HRP, horseradish peroxidase; KCN, potassium cyanide; LED, light-emitting diode; NIR, near-infrared; PBS, phosphate-buffered saline; ROS, reactive oxygen species; RT, room temperature; ssDNA, single-stranded DNA.

0306-4522/06$30.00+0.00 © 2006 Published by Elsevier Ltd on behalf of IBRO.
doi:10.1016/j.neuroscience.2005.12.047

Key words: caspase-3, electronic microcopy, near-infrared light, ssDNA, ROS.

Low-energy laser irradiation in the far red to near-infrared (NIR) range is found to modulate various biological processes (Karu, 1999) by increasing mitochondrial respiration or ATP synthesis (Passarella et al., 1984; Morimoto et al., 1994; Karu et al., 1995; Yu et al., 1997a; Wilden and Karthein, 1998), facilitating wound healing (Conlan et al., 1996; Yu et al., 1997b; Sommer et al., 2001; Whelan et al., 2001) and promoting cell survival (Shefer et al., 2002). Possible mechanisms involve an acceleration of electron transfer in the respiratory chain and activation of photoacceptors, such as cytochrome oxidase, thus pointing to a particular role for mitochondria. Mitochondria are sensitive to irradiation with monochromatic NIR, 50% of which is reportedly absorbed in the liver by mitochondrial chromophores, such as cytochrome oxidase (Beauvoit et al., 1994).

Direct benefit of photobiomodulation on cytochrome oxidase activity was tested and confirmed in primary neurons functionally inactivated by tetrodotoxin (TTX) (Wong-Riley et al., 2001, 2005) or poisoned by potassium cyanide (KCN) (Wong-Riley et al., 2005), an irreversible inhibitor of cytochrome oxidase. Photobiomodulation also has therapeutic benefit on rat retinal neurons poisoned by methanol-induced formate (Eells et al., 2003), a reversible inhibitor of cytochrome oxidase. Thus, NIR via light-emitting diode (LED) treatment appears to compete with inhibitors of cytochrome oxidase in activating this enzyme, resulting in increased enzyme activity, increased ATP production, and increased metabolic activity of neurons (Wong-Riley et al., 2005). The ability of LED pretreatment to reduce the number of cell deaths caused by KCN or azide, another inhibitor of cytochrome oxidase, is particularly intriguing (Wong-Riley et al., 2005) and deserves further investigation.

Cyanide toxicity mediated through the inhibition of cytochrome oxidase causes histotoxic action (Mills et al., 1996; Lee et al., 1998; Bhattacharya and Lakshmana Rao, 2001) and compromises cellular energy status, resulting in cell death (Wong-Riley et al., 2005). However, cyanide can produce neuronal deaths either by apoptosis or necrosis, depending on its concentration (Li et al., 2002; Prabhakaran et al., 2004) or differential susceptibility of brain areas (Mills et al., 1999). Cyanide exposure reportedly produces primarily apoptosis in cortical neurons but necrosis in mesencephalic cells (Prabhakaran et al., 2002). Our previous studies on primary visual cortical neurons indicated that cyanide at different concentrations caused varying proportions of cell deaths

and that pretreatment with LED was effective in rescuing many neurons from dying (Wong-Riley et al., 2005). However, the mode of cell death was unclear.

The goal of the present study was to test our hypothesis that LED protects neurons from apoptotic cell death induced by 100–300 μM KCN. Various indicators of apoptosis were used to determine if apoptotic indices would be reduced by LED and to test for possible mechanisms of LED rescue. Moreover, the possibility that apoptosis occurred via a caspase-mediated pathway was investigated. Primary cultures of postnatal rat visual cortical neurons were used as our model.

EXPERIMENTAL PROCEDURES

All experiments were carried out in accordance with the U.S. National Institutes of Health Guide for the Care and Use of Laboratory Animals and the Medical College of Wisconsin regulations. All efforts were made to minimize the number of animals and their suffering.

Primary neuronal cultures

Sprague–Dawley rats (1-day-old) were anesthetized with CO_2, and brains were removed, placed in balanced salt solution (Invitrogen, Carlsbad, CA, USA) and dissected. Meninges and surface blood vessels were stripped, visual cortices were minced into 1 mm^3 pieces and digested with 0.75% trypsin at 37 °C for 15 min. Cells were mechanically dissociated, and plated on poly-L-lysine-(Sigma, St. Louis, MO, USA) coated coverslips at a density of 5×10^5 cells/ml. The medium was changed to Neurobasal/B27 supplement (Invitrogen) and the cultures were maintained at 37 °C with 5% CO_2 in a humidified incubator. Cytosine arabinoside (Ara-C) (Sigma) was added on the second day of plating neurons to inhibit the replication of non-neuronal cells. Neuronal cultures were maintained by replacing half of the medium every five days. In this culture system, 95% of the cell population were neurons (Zhang and Wong-Riley, 1999).

Culture treatments

Experiments were carried out on 7–10 day old cultures of visual cortical neurons, with or without 670 nm LED pretreatment for 10 min at a power intensity of 50 mW/cm^2, giving a total energy density of 30 J/cm^2. An LED array (25 cm×10 cm) with a peak wavelength at 670 nm (Quantum Devices, Inc. Barnaveld, WI, USA) was placed beneath the covered culture dish of 60 mm diameter, with the room light turned off and irradiated accordingly. Cells were subdivided into eight groups: 1) cells pretreated with LED and then exposed to 100 μM KCN for 28 h; 2) cells exposed to 100 μM KCN for 28 h only; 3) cells pretreated with LED and then exposed to 300 μM KCN for 28 h; 4) cells exposed to 300 μM KCN for 28 h only; 5) normal cells treated with LED for 10 min and assayed 24 h later; 6) cells exposed to 1 mM KCN for 28 h; 7) cells exposed to caspase inhibitor I (at 1 μM, 3 μM, 5 μM, 7 μM, and 10 μM concentrations; Calbiochem, San Diego, CA, USA) in the medium for 30 min before exposure to 300 μM KCN for 28 h; and 8) normal cells without exposure to KCN or treatment with LED as normal controls.

Electron microscopy

Cultures were fixed at 4 °C in a solution of 4% paraformaldehyde and 0.1% glutaraldehyde in 0.1 M phosphate buffer (PB), pH 7.2 and 4% sucrose for 1 h. After washing in phosphate-buffered saline (PBS), they were postfixed with 1% osmium tetroxide for 30 min, dehydrated in an ascending series of alcohol, and embedded in Durcupan (Sigma). Ultrathin sections were cut and collected on 200-mesh grids (Electron Microscopy Sciences, Hatfield, PA, USA). Grids were post-stained with 2% uranyl acetate at 37 °C for 30 min and 2.5% Reynold's lead citrate at room temperature (RT) for 25 min and examined with a JEOL 100CX transmission electron microscope.

Nuclear (DNA) staining

To quantify and assess nuclear morphology, cortical neurons were fixed with 2% paraformaldehyde in PBS (pH 7.4) followed by cold methanol at RT. After washing with PBS, cultures were stained for 15 min with 1 μg/ml of the fluorescent DNA-binding dye Hoechst 33258 (Sigma) to reveal nuclear condensation or aggregation, as described previously (Zhang et al., 2000). Hoechst-stained cells were visualized and photographed using the BA450 filter under the fluorescent microscope (Nikon). Five hundred to 1000 cells in five to 10 separate fields of each coverslip in each group were counted, and counts were made under the same treatment condition and repeated at least three times.

Single-stranded DNA (ssDNA) immunostaining

Immunolabeling of ssDNA was performed as described by Frankfurt and colleagues (Frankfurt et al., 1996; Frankfurt and Krishan, 2001a,b) with slight modifications. Cells were washed in PBS, pH 7.4 at 4 °C and re-fixed in methanol/PBS (4:1, vol/vol) at −20 °C. Coverslips were heated to 75 °C for 20 min in an oven and cooled for 4 min at 4 °C with formamide. After blocking with 3% nonfat dry milk at 37 °C for 1 h, cells were incubated with anti-ssDNA monoclonal antibodies MAB 3299 (Chemicon, Temecula, CA, USA) at 1:200 dilution for 40 min. This was followed by secondary goat-anti-mouse antibodies conjugated to horseradish peroxidase (HRP) (Bio-Rad, Hercules, CA, USA) at 1:100 dilution for 30 min at RT. The labeling was visualized by the 3,3′-diaminobenzidine (DAB) (Sigma) reaction. Finally, cells were stained with hematoxylin (Sigma) at RT for 30 s and differentiated in 1% hydrochloric acid in 70% alcohol for 10 s. Nuclear labeling of ssDNA-positive cells and normal cells were counted (~500–1000 cells per group), and counts were made in at least five separate fields per treatment condition. The experiment was repeated at least three times.

Immunocytochemistry for active caspase-3, Bax, and Bcl-2

Neurons were washed with PBS and fixed with 4% paraformaldehyde in 0.1 M sodium phosphate buffer (pH 7.4) for 30 min on ice. After blocking non-specific binding with 2% H_2O_2 for 30 min, and 1% bovine serum albumin with 4% normal goat serum (NGS) for 1 h, cells were incubated with polyclonal antibodies against active caspase-3 (Chemicon) at 1:200 dilution; monoclonal antibodies against Bax or Bcl-2 (Santa Cruz Biotechnology, Santa Cruz, CA, USA) at 1:200 dilution (for both) overnight at 4 °C. This was followed by goat-anti-rabbit (Bio-Rad) or goat-anti-mouse secondary antibodies conjugated to HRP at 1:100 dilution for 2 h at RT. The labeling of cytoplasm was visualized by using the DAB reaction.

Optical densitometry analysis

To analyze quantitative changes in active caspase-3, Bax, and Bcl-2 immunoreactivity following different treatments, optical densities of reaction product were measured by means of a Zonax MPM03 photometer (Zeiss, Thornwood, NY, USA) attached to a Zeiss compound microscope. Measurements were used with a 25× objective and a spot size of 2 μm diameter directed at the centers of cytoplasm of individual neurons. Possible variations in coverslip and slide thickness were negated by adjusting a blank region of each coverslip/slide to zero. For each experiment of

each treatment group, readings were taken from 100 to 200 cells in five random fields. The mean value±S.E.M. of reaction product in each study were based on three independent experiments.

Western blots

Control and experimental samples were lysed with lysis buffer (0.5% Triton X-100 and 5 mM EDTA) and centrifuged for 10 min at 15,000×*g* at 4 °C. The concentration of supernatant was measured with Bio-Rad protein Assay Kit Π (Bio-Rad). Total proteins (50 μg) were loaded onto 10% SDS-PAGE gels. After SDS-PAGE, proteins were electrophoretically transferred onto polyvinylidene difluoride (PVDF) membranes (Bio-Rad). After blocking, cells were incubated with primary antibodies (polyclonal antibodies against active caspase-3 at 1:1000 dilution; monoclonal antibodies against Bax or Bcl-2 at 1:100 dilution; monoclonal antibodies against β-actin Σ at 1:3000 dilution) for 1 h at RT, blots were washed and incubated in horseradish-peroxidase-conjugated secondary goat-anti-rabbit or goat-anti-mouse antibodies at 1:3000 dilution. Blots were then reacted with ECL solution, exposed to autoradiographic film (Amersham, Piscataway, NJ, USA) for visualization of immunoreactive bands. Intensities of immunoreactive bands were measured with an Alpha Imager (Alpha Innotech, San Leandro, CA, USA). Relative changes of each reaction were normalized with β-actin. Each experiment was repeated at least three times.

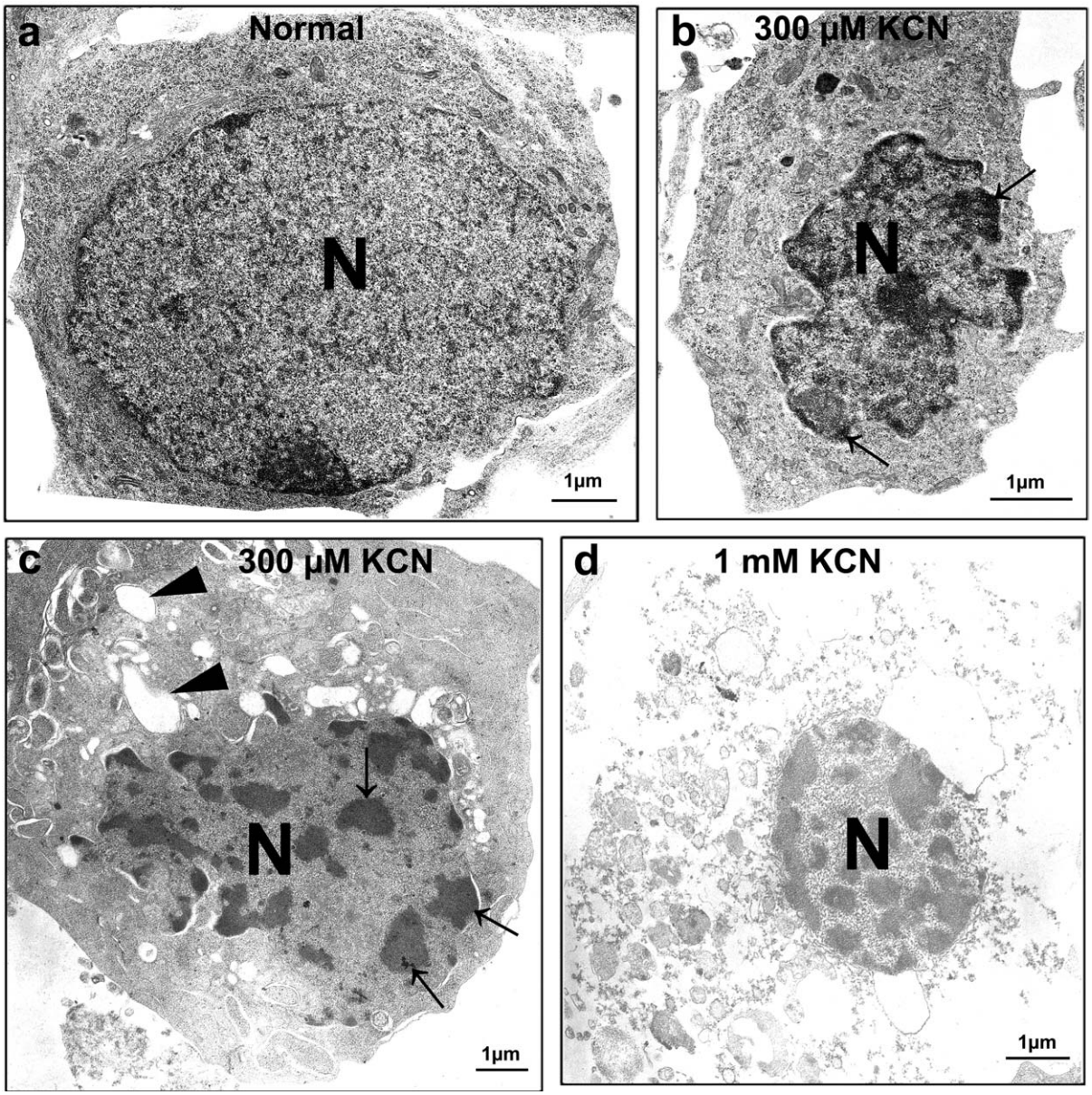

Fig. 1. Ultrastructural morphology of primary neurons with or without KCN exposure. (a) Normal (control) neurons show normal-sized nuclei with homogeneously dispersed chromatin, normal cytoplasmic organelles including mitochondria, and intact plasma membrane. When exposed to 300 μM KCN, many cells exhibited characteristic apoptotic changes with nuclear condensation (b) or nuclear fragmentations (c, arrows) and cytoplasmic vacuole formation (c, arrowheads), but the cytoplasmic and nuclear membranes remained intact. (d) With 1 mM KCN exposure, most neurons underwent necrosis with nuclear fragmentation, disintegration and loss of cytoplasmic organelles, swelling of mitochondria, and disintegration of the plasma membrane. N, nucleus. Scale bar=1 μm for a–d.

Measurement of intracellular reactive oxygen species (ROS)

ROS levels were determined by using 5-(and -6) chloromethy-2′, 7-dichlorodihydrofluorescein diacetate acetyl ester (CM-H_2DCFDA, Molecular Probes, Inc., Eugene, OR, USA). Control and treated neurons were washed with warmed balanced salt solution and incubated with 2 μM CM-H_2DCFDA in balanced salt solution for 20 min at 37 °C. After washing, cells were switched to normal growth medium and viewed with a Nikon fluorescent microscope. The fluorescence intensity was measured by using the NIH ImageJ software ij134.

Statistics

Tukey or ANOVA and two-tailed Student's *t*-test were used for paired comparisons and analysis of variance for group differences between treated and untreated ones. A *P* value of 0.05 or less was considered significant.

RESULTS

Morphological changes evaluated by transmission electron microscopy

Primary neuronal cultures showed normal-sized nuclei with homogeneously dispersed chromatin (euchromatin), cytoplasm with usual organelles including mitochondria, and intact plasma membrane (Fig. 1a). When exposed to 300 μM KCN, many neurons exhibited nuclear shrinkage and condensation with or without chromatin aggregation and vacuole formation in the cytoplasm; however, their cytoplasmic and nuclear membranes remained intact, characteristic of apoptosis (Fig. 1b and c). With 1 mM KCN exposure, on the other hand, most neurons displayed nuclear condensation and fragmentation, disintegration of cytoplasm, swelling

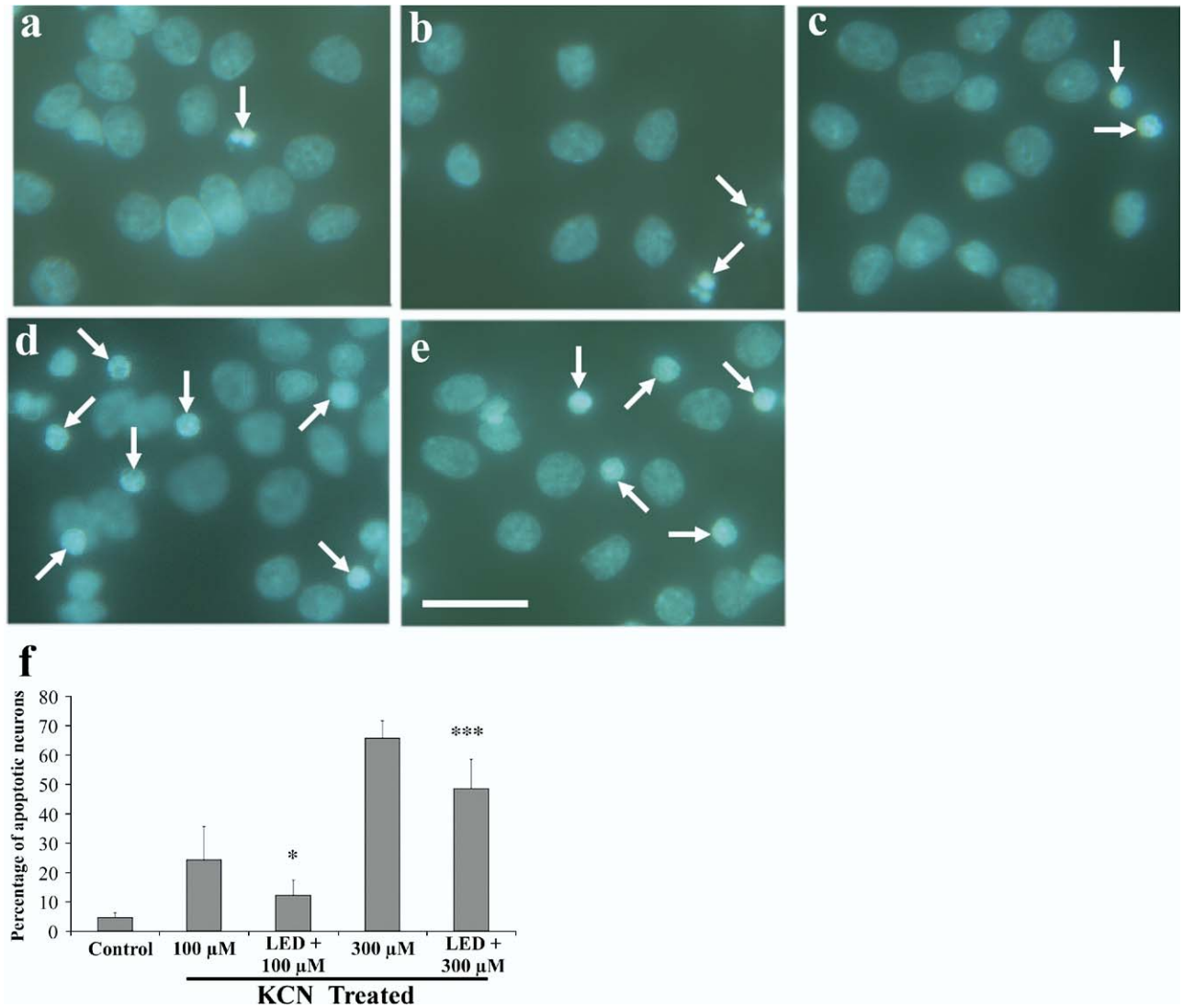

Fig. 2. Hoechst staining of cultured neurons exposed to KCN or pretreated with LED. (a) Control; b: 100 μM KCN; c: LED plus 100 μM KCN; d: 300 μM KCN; e: LED plus 300 μM KCN. Apoptotic neurons (arrows) showed condensation or decreased nuclear size, with or without nuclear fragmentation. Scale bar=35 μm for a–e. (f) Quantification of apoptotic neurons (from a–e) as percentage of normal cells in each group. LED pretreatment significantly reduced the percentage of apoptotic neurons as compared with non-treated ones in the 100 μM KCN group (* $P<0.05$) and the 300 μM KCN group ($P<0.001$). All treatments are significantly different from controls (*** $P<0.001$).

of mitochondria, loss of organelles, and disintegration of the plasma membrane characteristic of necrosis (Fig. 1d).

Effects of LED on apoptotic neurons revealed by Hoechst 33258 staining

Primary visual cortical neurons from control (normal) cultures showed normal nuclei and homogeneously dispersed chromatin with the Hoechst 33258 stain (Fig. 2a). When exposed to 100–300 μM KCN, many neurons exhibited apoptotic nuclear morphology with condensed chromatin, reduced nuclear size and/or nuclear fragmentation (Fig. 2b, d). Pretreatment of neurons with LED for 10 min (total energy density of 30 J/cm^2) before exposure to 100 or 300 μM KCN significantly reduced the number of cells with apoptotic nuclear morphology (Fig. 2c, e). The percent of apoptotic cells decreased from 24.4% (with 100 μM KCN) to 12.3% (100 μM KCN plus LED) ($P<0.05$), and from 65.9% (with 300 μM KCN) to 48.7% (300 μM KCN plus LED) ($P<0.001$), representing a 49.6% and 26.1% reduction, respectively, in each group (Fig. 2f).

Effects of LED on ssDNA positive neurons

Control (normal) visual cortical neurons showed normal-sized nuclei, with very few neurons (5.3%) exhibiting relatively

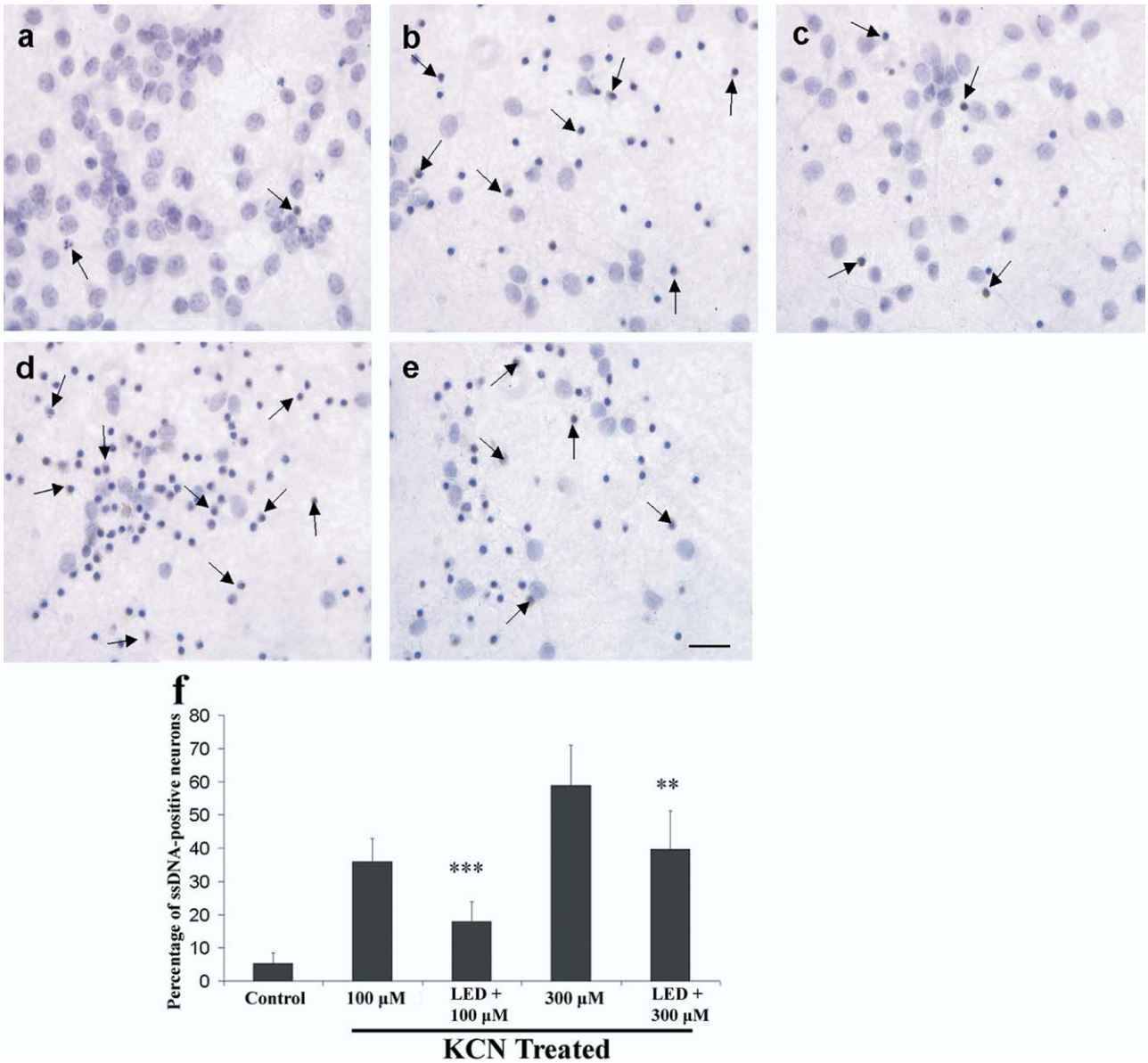

Fig. 3. ssDNA, immunostaining of cultured neurons exposed to KCN or pretreated with LED. Nuclei were doubly stained with DAB (for ssDNA; arrows) and hematoxylin (for all neurons). (a) Control; b: 100 μM KCN; c: LED plus 100 μM KCN; d: 300 μM KCN; e: LED plus 300 μM KCN. KCN significantly increased the number of ssDNA-positive neurons (b and d), but LED pretreatment substantially reduced that number (c and e). Scale bar=35 μm for a–e. (f) Quantification of ssDNA-positive neurons as percentage of normal cells in each group. LED pretreatment significantly reduced the percentage of apoptotic neurons in the100 μM KCN (*** $P<0.001$) and the 300 μM KCN (** $P<0.01$) groups as compared with their untreated counterparts. All treatments are significantly different from controls ($P<0.001$).

small nuclear size that were labeled with ssDNA in the nucleus (arrows, Fig. 3a). Exposure to KCN resulted in an increasing number of neurons with ssDNA labeling, condensed chromatin, reduced nuclear size, and increased nuclear fragmentation (arrows, Fig. 3b, d). Pretreatment with LED for 10 min before exposure to 100–300 μM KCN significantly reduced the number of neurons with apoptotic nuclear morphology (arrows, Fig. 3c, e). With 100 μM KCN exposure, LED pretreatment reduced the number of ssDNA-positive neurons from 36% to 17.9%, equivalent to a 50.3% reduction ($P<0.001$). With 300 μM KCN, LED pretreatment decreased the percentage from 58.9% to 39.6%, representing a 32.8% reduction ($P<0.01$) (Fig. 3f).

Effects of LED on active caspase-3 protein expression

Active caspase-3 activity in the cytoplasm is a good indicator of cellular apoptotic status (Kiang et al., 2003). Immunocytochemical labeling showed that active caspase-3 was mainly in the cytoplasm. Control neurons had very low immunoreactivity, but caspase-3 immunoreactivity was significantly increased with KCN exposure (Fig. 4a–e) ($P<0.001$ for both groups). These values were significantly reduced with LED pretreatment, in the presence of 100 μM KCN ($P<0.05$) or 300 μM KCN ($P<0.001$) (Fig. 4g).

Active caspase-3 protein levels were also demonstrated with Western blots. Control cells showed a weak band, but the density significantly increased with KCN exposure ($P<0.001$). With LED pretreatment, the levels of immunoreactivity were significantly lower than those without the pretreatment in the presence of 100 or 300 μM KCN ($P<0.05$ for both group) (Fig. 4f, h). These results were consistent with the caspase-3 immunohistochemical results.

Effect of caspase inhibitor I on cultured neurons exposed to KCN

To determine the role of caspase in the apoptotic pathway of cells exposed to 300 μM KCN, caspase inhibitor I at 1,

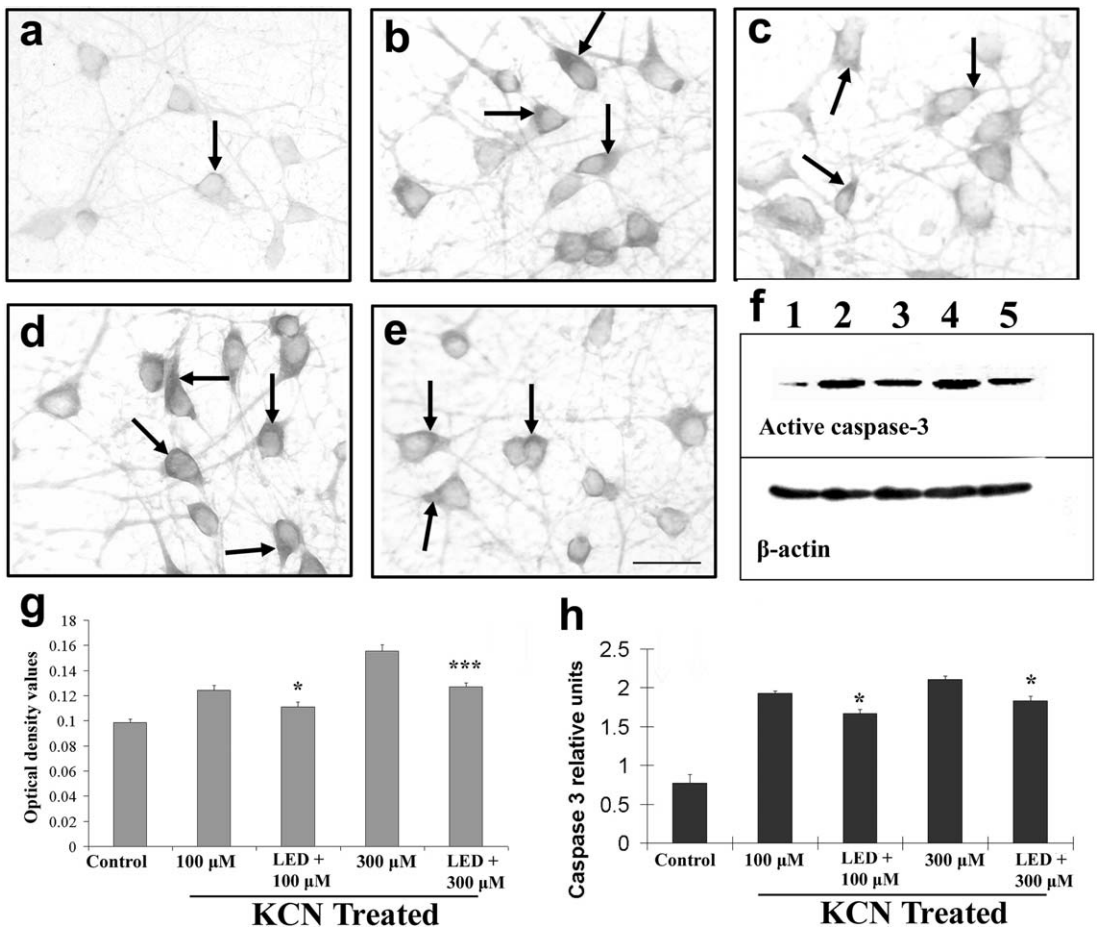

Fig. 4. Changes in active caspase-3 protein levels in neurons exposed to KCN or pretreated with LED. (a–e) Immunohistochemistry; f, Western blots. (a and lane 1 in f) Control; b and lane 2 in f: 100 μM KCN; c and lane 3 in f: LED plus 100 μM KCN; d and lane 4 in f: 300 μM KCN; e and lane 5 in f: LED plus 300 μM KCN. Active caspase-3 immunoreactivity in the cytoplasm (arrows) increased significantly with increasing KCN concentration, but LED pretreatment decreased the intensity of immunoreactivity. Scale bar=35 μm for a–e. (g) Optical densitometric measurements of active caspase-3 immunoreactivity. The values were significantly increased by KCN ($P<0.05$–0.001), but LED pretreatment reduced the values in the presence of 100 μM KCN (* $P<0.05$) and 300 μM KCN (*** $P<0.001$) as compared with their untreated counterparts. (h) Quantitative analysis of relative changes in active caspase-3 protein levels detected in Western blots. Caspase-3 levels were significantly increased by KCN ($P<0.001$ for all) and significantly reduced by LED pretreatment. (* $P<0.05$ for both 100 μM and 300 μM KCN).

3, 5, 7, and 10 μM concentrations were applied to cells for 30 min before exposure to 300 μM KCN for 28 h. Apoptotic and normal neurons were visualized with the Hoechst 33258 stain and counted under the fluorescent microscope. Results indicated that caspase inhibitor I pretreatment significantly decreased the number of apoptotic neurons induced by 300 μM KCN, representing a 15.3%, 18.6%, 18.9%, 34.4%, and 39.6% reduction, respectively, in the various concentrations of caspase inhibitor I tested ($P<0.01$ for 1, 3, and 5 μM of inhibitor, and $P<0.001$ for 7 and 10 μM of inhibitor) (Fig. 5).

Effects of LED on Bax and Bcl-2 protein expression

Bax and Bcl-2 protein levels were measured by immunohistochemistry and Western blots. Bax expression was up-regulated by KCN exposure and was concentration-dependent. The value reached high significance with 300 μM KCN ($P<0.001$). LED pretreatment reduced all Bax expressions to control levels in the presence of 100 or 300 μM KCN (Fig. 6a, c, e). In contrast to Bax, Bcl-2 protein level was down-regulated by KCN, and reached statistical significance at 300 μM KCN concentration ($P<0.001$ and $P<0.01$ for immunohistochemical and Western blot results, respectively, as compared with controls). Pretreatment with LED up-regulated Bcl-2 expression to control levels in the presence of 100–300 μM KCN (Fig. 6b, d, f). LED treatment alone for 10 min without KCN exposure did not change the levels of Bax or Bcl-2 proteins that were significantly different from controls (data not shown).

Effects of LED on ROS generation in neurons

To determine the extent of ROS generation in neurons exposed to 300 μM KCN, fluorescence intensity of CM-H_2DCFDA, a marker of ROS, was evaluated in four groups of cells: normal (control), normal plus 10 min of LED, 300 μM KCN for 28 h, and pretreatment with LED for 10 min before 300 μM KCN for 28 h (Fig. 7). KCN exposure significantly increased the intensity of CM-H_2DCFDA expression ($P<0.001$). With LED pretreatment, the fluorescent signal was significantly lower than that without the pretreatment ($P<0.05$) (Fig. 7g, h, and i). Under normal conditions, LED treatment for 10 min did not cause significant changes in ROS levels as compared with controls (Fig. 7e, f, and i).

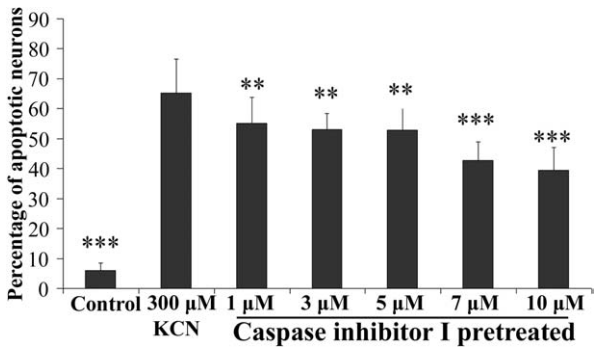

Fig. 5. Primary neurons exposed to 300 μM KCN with or without caspase inhibitor I pretreatment. Apoptotic neurons were shown by Hoechst stain. Caspase inhibitor I pretreatment significantly decreased the percentage of apoptotic neurons. All statistical comparisons were with the 300 μM KCN group without LED pretreatment. ** $P<0.01$, *** $P<0.001$.

DISCUSSION

The present study demonstrates the protective role of LED-mediated NIR pretreatment against KCN-induced apoptosis in cultured rat cortical neurons. Apoptosis in the presence of 300 μM KCN was verified by electron microscopy, Hoechst 33258, ssDNA, Bax, and active caspase-3. Necrosis did not occur at the dosages used in conjunction with LED, but it did with 1 mM of KCN. Apoptosis from 100 to 300 μM KCN exposure involves the induction of active caspase-3, the pro-apoptotic Bax protein, and ROS. LED pretreatment for only 10 min at 30 J/cm^2 energy density was able to rescue a significant number of neurons from undergoing the apoptotic pathway and significantly up-regulated the anti-apoptotic protein Bcl-2 suppressed by KCN.

Apoptosis is a mechanism of cell death that includes a network of metabolic events triggered by a variety of biological and physical stimuli. The death process is characterized by selective proteolysis of cytoplasmic and nuclear substrates that disable homeostatic and repair processes and mediate structural disassembly and morphological changes (Wu et al., 2002). Internucleosomal cleavage and condensed chromatin or reduced nuclear size are characteristics of apoptosis. A combination of methods used in the present study verified that apoptotic cell death induced by KCN is dose-dependent, and that LED pretreatment effectively rescues a large percentage of neurons from cyanide-induced apoptosis.

ssDNA is a specific and sensitive marker of apoptotic cell death (Watanabe et al., 1999; Frankfurt and Krishan, 2001a,b). ssDNA is the product of apoptosis, and is based on the action of endonuclease on DNA. It is a convenient and effective way to detect *in situ* apoptosis immunohistochemically (Watanabe et al., 1999). Among the five methods [ssDNA-staining, poly-(ADP-ribose)-polymerase-(PARP) cleavage, TUNEL-reaction, annexin-V-binding, and Apo-2.7-expression], only ssDNA-staining allows the complete differentiation of apoptosis from necrosis, and is thus suitable for a reliable detection of early as well as late apoptosis (Zhao et al., 2003). TUNEL-reaction is not specific for apoptosis, as it also detects necrotic and autolytic types of cell death (Gold et al., 1994; Grasl-Kraupp et al., 1995; Baima and Sticherling, 2002). The number of ssDNA-positive neurons increased significantly with exposure to 100 or 300 μM KCN for 28 h, confirming that, within these dosages used, neurons die via the apoptotic pathway. With LED pretreatment, the number of ssDNA-positive neurons was significantly lower than that without the pretreatment, consistent with our hypothesis that LED rescues neurons from apoptosis.

Among the apoptotic pathways, the intrinsic (mitochondria) one is one of the major pathways for caspase activa-

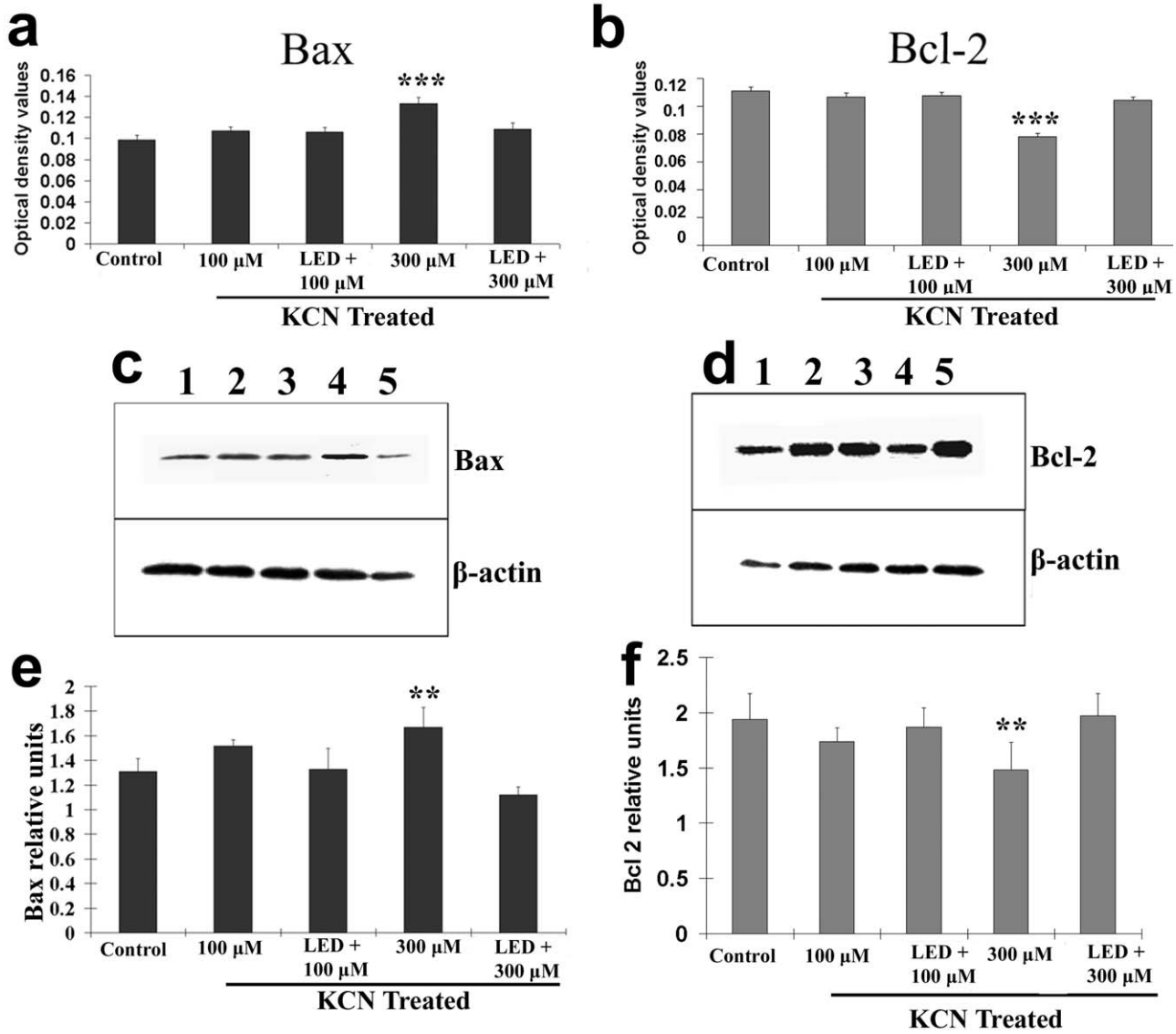

Fig. 6. Optical densitometric quantification of changes in Bax and Bcl-2 protein levels in neurons exposed to KCN with or without LED pretreatment. (a) Bax immunoreactivity was significantly increased in cells exposed to 300 μM KCN (*** $P<0.001$), but reduced to control levels by LED pretreatment. (b) Bcl-2 expression was significantly down-regulated by 300 μM KCN (*** $P<0.001$), but LED pretreatment raised this value to control levels. Western blot analysis of Bax (c) and Bcl-2 (d). Lane 1: control; lane 2: 100 μM KCN; lane 3: LED plus 100 μM KCN; lane 4: 300 μM KCN; lane 5: LED plus 300 μM KCN. (e, f) Quantitative analyses of Western blots. 300 μM KCN exposure significantly increased Bax (** $P<0.01$) but decreased Bcl-2 (** $P<0.01$) expression. LED pretreatment restored each to control values.

tion. Caspase-3 is a potent effector of apoptosis and is triggered via several different pathways in a variety of mammalian cell types. In its active form, caspase-3 plays a role in the proteolytic cleavage of proteins, such as the cleavage of nuclear DNA repair enzyme poly (ADP-ribose) polymerase and inhibitor of caspase-activated DNase (Matsuu et al., 2003). The present study demonstrates that caspase-3 expression was increased in rat visual cortical neurons after exposure to 100–300 μM KCN, and that LED pretreatment reduces the severity of caspase-3 activation. Thus, the progression of KCN-induced apoptosis in cultured neurons was correlated temporally with caspase-3 up-regulation, and LED pretreatment partially protects against KCN-induced apoptosis. Moreover, caspase inhibitor I significantly reduced the number of neurons undergoing apoptosis in a concentration-dependent manner, indicating that KCN-induced apoptosis involves a caspase-associated pathway. However, up to 10 μM of caspase inhibitor I did not abolish apoptosis completely. This may mean that: a) a higher concentration of inhibitors is needed; b) 300 μM of KCN is too potent for caspase inhibitors to prevent exceptionally vulnerable neurons from dying; and/or c) factors other than caspases may also be involved in KCN-induced apoptosis.

Programmed cell death was regulated by pro and anti-apoptotic Bcl-2 family of proteins, and over-expression of anti-apoptotic proteins (Bcl-2) prevents the release of cytochrome c from mitochondria in the caspase cascade of

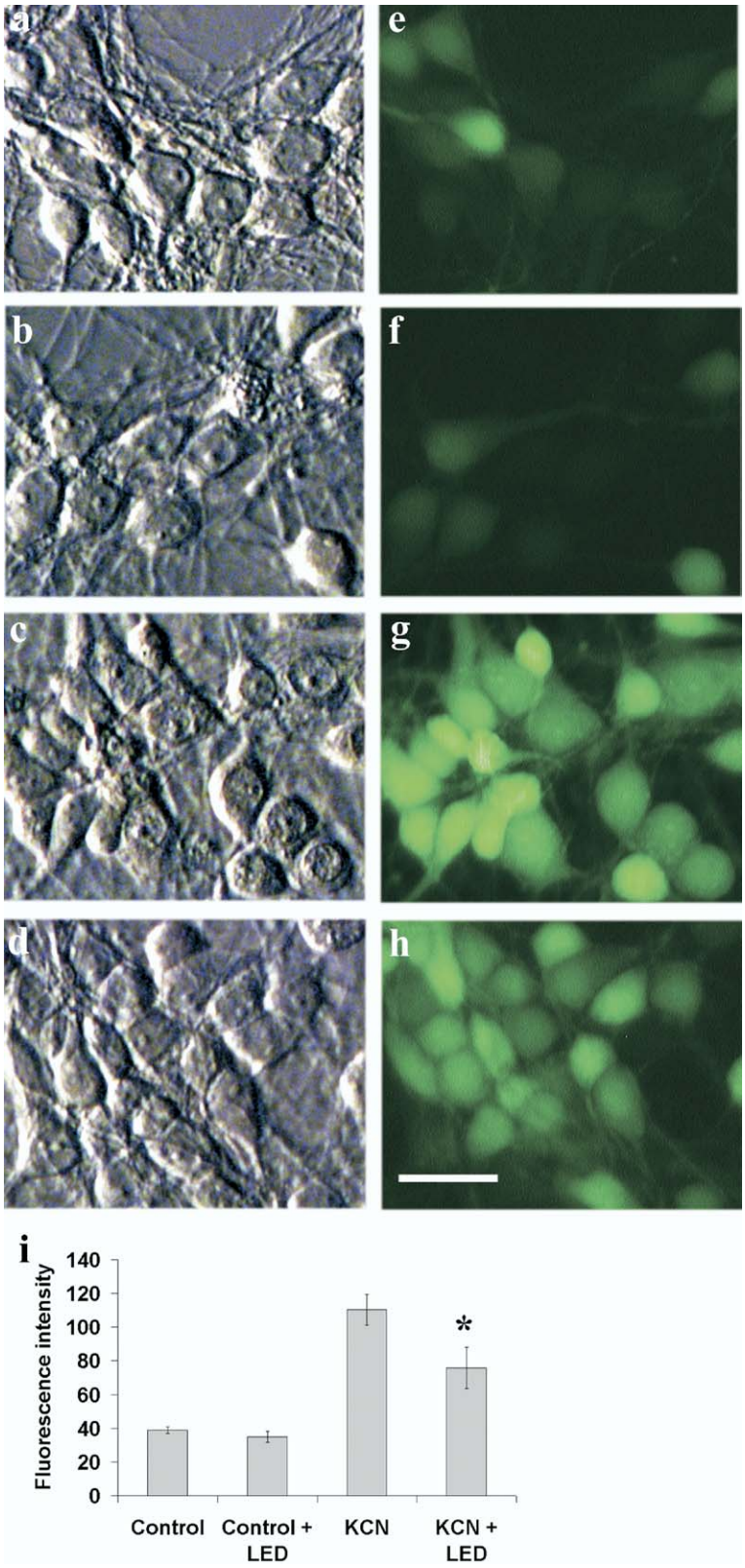

Fig. 7. ROS measurement by CM-H_2DCFDA fluorescence in normal and KCN exposed neurons with or without LED pretreatment. (a–d) Phase contrast. (e–h) Same fields as a–d, respectively, with CM-H_2DCFDA fluorescence. (a, e) Normal control; b and f: normal neurons exposed to LED for 10 min and tested 24 h later; c and g: 300 μM KCN for 28 h; d and h: LED pretreatment for 10 min followed by 300 μM KCN for 28 h. CM-H_2DCFDA expression was increased by KCN exposure (g), but the fluorescent signal was much lower in the LED-pretreated (h) as compared with non-pretreated ones (g) in the presence of 300 μM KCN. Under normal conditions, LED treatment for 10 min (f) did not induce a significant change in CM-H_2DCFDA expression as compared with controls (e). Scale bar=30 μm for a–h. (i) Quantitative analyses of ROS expression. LED pretreatment exhibited a significantly lower CM-H_2DCFDA fluorescent value as compared with non-pretreated cells in the presence of 300 μM KCN (* $P<0.05$).

apoptotic cell death after cytotoxic insults (Desagher and Martinou, 2000). Over-expression of Bax, or an increase in the ratio of Bax to Bcl-2, however, is associated with programmed cell death (Oltvai et al., 1993). The present data indicate that there was a significant increase in Bax expression and a significant decrease in Bcl-2 expression in neurons exposed to 300 μM KCN, and that LED pretreatment effectively reversed these trends to control levels. These findings are consistent with changes in active caspase-3 protein levels. Our results are also consistent with the up-regulation of Bcl-2 and down-regulation of Bax expression associated with various protective measures against apoptosis in neuronal cultures (Zhang et al., 2003; Zhao et al., 2004). Other pro- and anti-apoptotic proteins may also be involved in the KCN-exposed and LED treated conditions.

Cyanide-mediated inhibition of cytochrome c oxidase leads to decreased mitochondrial membrane potential and enhanced ROS generation (Gunasekar et al., 1998; Prabhakaran et al., 2002, 2004; present study). Excessive ROS contributes to mitochondrial dysfunction and signals the initiation of cell death (Carmody and Cotter, 2001; Kitazawa et al., 2002). LED pretreatment significantly reduces ROS generation in KCN-poisoned neurons (present study). This response is triggered, at least in part, by KCN, as LED does not cause any change in ROS levels in neurons under normal conditions (present study).

Cells undergoing apoptosis also suffer from reduced ATP content (Hiura et al., 2000; Comelli et al., 2003; Atlante et al., 2005). Likewise, KCN also induces a significant reduction in cellular ATP content that is rescued by LED treatment (Wong-Riley et al., 2005). This is consistent with the known benefit of NIR light in increasing ATP synthesis (Passarella et al., 1984; Morimoto et al., 1994; Karu et al., 1995; Yu et al., 1997a; Wilden and Karthein, 1998).

Of the three major photoacceptor molecules known to absorb light in the NIR range: hemoglobin, myoglobin, and cytochrome oxidase, only cytochrome c oxidase (EC1.9.3.1) has been associated with energy production. Our previous findings also suggest that LED (670 nm) directly stimulates cytochrome oxidase in cellular energy metabolism in both normal and KCN-poisoned neurons (Wong-Riley et al., 2001; 2005). Thus, LED most likely up-regulates both the activity and synthesis of cytochrome oxidase, resulting in increased energy production in neurons.

The fact that 10 min of LED pretreatment results in a significant rescue of neurons from KCN-induced apoptosis strongly suggests that a cascade of events has been induced to activate or repress a variety of genes. Indeed, our preliminary data from neurons as well as our published report on wound healing in diabetic mice indicate specific up- and down-regulation of different genes by LED (Wong-Riley et al., 2002; Whelan et al., 2003). The molecular signal(s) that mediate(s) these changes awaits further investigation (see Discussion in Wong-Riley et al., 2005).

CONCLUSION

In summary, our results demonstrate that at the dosages used, cyanide induces cell death via the apoptotic pathway in primary cultures of rat visual cortical neurons. LED pretreatment for 10 min (at a total energy density of 30 J/cm^2) significantly decreases KCN-induced apoptosis in these neurons, most likely via a mechanism that involves the reduction of ROS generation, the down-regulation of apoptotic proteins, the up-regulation of anti-apoptotic proteins, as well as the previously reported activation of cytochrome oxidase and energy metabolism. The prevention of apoptosis by LED is not complete, due to the potent inhibition of cytochrome oxidase by cyanide.

REFERENCES

Atlante A, Giannattasio S, Bobba A, Gagliardi S, Petragallo V, Calissano P, Marra E, Passarella S (2005) An increase in the ATP levels occurs in cerebellar granule cells en route to apoptosis in which ATP derives from both oxidative phosphorylation and anaerobic glycolysis. Biochim Biophys Acta 1708:50–62.

Baima B, Sticherling M (2002) How specific is the TUNEL reaction? An account of a histochemical study on human skin. Am J Dermatopathol 24:130–134.

Beauvoit B, Kitai T, Chance B (1994) Contribution of the mitochondrial compartment to the optical properties of the rat liver: a theoretical and practical approach. Biophys J 67:2501–2510.

Bhattacharya R, Lakshmana Rao PV (2001) Pharmacological interventions of cyanide-induced cytotoxicity and DNA damage in isolated rat thymocytes and their protective efficacy in vivo. Toxicol Lett 119:59–70.

Carmody RJ, Cotter TG (2001) Signalling apoptosis: a radical approach. Redox Rep 6:77–90.

Comelli M, Di Pancrazio F, Mavelli I (2003) Apoptosis is induced by decline of mitochondrial ATP synthesis in erythroleukemia cells. Free Radic Biol Med 34:1190–1199.

Conlan MJ, Rapley JW, Cobb CM (1996) Biostimulation of wound healing by low-energy laser irradiation. J Clin Periodontol 23: 492–496.

Desagher S, Martinou JC (2000) Mitochondria as the central control point of apoptosis. Trends Cell Biol 10:369–377.

Eells JT, Henry MM, Summerfelt P, Wong-Riley MTT, Buchmann EV, Kane M, Whelan NT, Whelan HT (2003) Therapeutic photobiomodulation for methanol-induced retinal toxicity. Proc Natl Acad Sci U S A 100:3439–3444.

Frankfurt OS, Robb JA, Sugarbaker EV, Villa L (1996) Monoclonal antibody to single-stranded DNA is a specific and sensitive cellular marker of apoptosis. Exp Cell Res 226:387–397.

Frankfurt OS, Krishan A (2001a) Identification of apoptotic cells by formamide-induced DNA denaturation in condensed chromatin. J Histochem Cytochem 49:369–378.

Frankfurt OS, Krishan A (2001b) Enzyme-linked immunosorbent assay (ELISA) for the specific detection of apoptotic cells and its application to rapid drug screening. J Immunol Methods 253: 133–144.

Gold R, Schmied M, Giegerich G, Breitschopf H, Hartung HP, Toyka KV, Lassmann H (1994) Differentiation between cellular apoptosis and necrosis by the combined use of in situ tailing and nick translation techniques. Lab Invest 71:219–225.

Grasl-Kraupp B, Ruttkay-Nedecky B, Koudelka H, Bukowska K, Bursch W, Schulte-Hermann R (1995) In situ detection of fragmented DNA (TUNEL assay) fails to discriminate among apoptosis, necrosis, and autolytic cell death: a cautionary note. Hepatology 21: 1465–1468.

Gunasekar PG, Borowitz JL, Isom GE (1998) Cyanide-induced generation of oxidative species: involvement of nitric oxide synthase and cyclooxygenase-2. J Pharmacol Exp Ther 285:236–241.

Hiura TS, Li N, Kaplan R, Horwitz M, Seagrave JC, Nel AE (2000) The role of a mitochondrial pathway in the induction of apoptosis by chemicals extracted from diesel exhaust particles. J Immunol 165:2703–2711.

Karu T (1999) Primary and secondary mechanisms of action of visible to near-IR radiation on cells. J Photochem Photobiol B 49:1–17.

Karu T, Pyatibrat L, Kalendo G (1995) Irradiation with He-Ne laser increases ATP level in cells cultivated in vitro. J Photochem Photobiol B Biol 27:219–223.

Kiang JG, Warke VG, Taokos GC (2003) NaCN-induced chemical hypoxia is associated with altered gene expression. Mol Cell Biochem 254:211–216.

Kitazawa M, Wagner JR, Kirby ML, Anantharam V, Kanthasamy AG (2002) Oxidative stress and mitochondrial-mediated apoptosis in dopaminergic cells exposed to methylcyclopentadienyl manganese tricarbonyl. J Pharmacol Exp Ther 302:26–35.

Lee MM, Hseih MT, Kuo JS, Yeh FT, Huang HM (1998) Magnolol protects cortical neuronal cells from chemical hypoxia in rats. Neuroreport 9:3451–3456.

Li L, Prabhakaran K, Shou Y, Borowitz JL, Isom GE (2002) Oxidative stress and cyclooxygenase-2 induction mediate cyanide-induced apoptosis of cortical cells. Toxicol Appl Pharmacol 185:55–63.

Matsuu M, Shichijo K, Okaichi K, Wen CY, Fukuda E, Nakashima M, Nakayama T, Shirahata S, Tokumaru S, Sekin I (2003) The protective effect of fermented milk kefir on radiation-induced apoptosis in colonic crypt cells of rats. J Radiat Res 44:111–115.

Mills EM, Gunasekar PG, Pavlakovic G, Isom GE (1996) Cyanide-induced apoptosis and oxidative stress in differentiated PC12 cells. J Neurochem 67:1039–1046.

Mills EM, Gunasekar PG, Li L, Borowitz JL, Isom GE (1999) Differential susceptibility of brain areas to cyanide involves different modes of cell death. Toxicol Appl Pharmacol 156:6–16.

Morimoto Y, Arai T, Kikuchi M, Nakajima S, Nakamura H (1994) Effect of low-intensity argon laser irradiation on mitochondrial respiration. Lasers Surg Med 15:191–199.

Oltvai ZN, Milliman CL, Korsmeyer SJ (1993) Bcl-2 heterodimerizes in vivo with a conserved homolog, Bax, that accelerates programmed cell death. Cell 74:609–619.

Passarella S, Casamassima E, Molinari S, Pastore D, Quagliariello E, Catalano IM, Cingolani A (1984) Increase of proton electrochemical potential and ATP synthesis in rat liver mitochondria irradiated in vitro by helium-neon laser. FEBS Lett 175:95–99.

Prabhakaran K, Li L, Borowitz JL, Isom GE (2002) Cyanide induces different modes of death in cortical and mesencephalon cells. J Pharmacol Exp Ther 303:510–519.

Prabhakaran K, Li L, Borowitz JL, Isom GE (2004) Caspase inhibition switches the mode of cell death induced by cyanide by enhancing reactive oxygen species generation and PARP-1 activation. Toxicol Appl Pharmacol 195:194–202.

Shefer G, Partridge TA, Heslop L, Gross JG, Oron U, Halevy O (2002) Low-energy laser irradiation promotes the survival and cell cycle entry of skeletal muscle satellite cells. J Cell Sci 115:1461–1469.

Sommer AP, Pinheiro AL, Mester AR, Franke RP, Whelan HT (2001) Biostimulatory windows in low-intensity laser activation: lasers, scanners, and NASA's light-emitting diode array system. J Clin Laser Med Surg 19:29–33.

Watanabe I, Toyoda M, Okuda J, Tenjo T, Tanaka K, Yamamoto T, Kawasaki H, Sugiyama T, Kawarada Y, Tanigawa N (1999) Detection of apoptotic cells in human colorectal cancer by two different in situ methods: antibody against single-stranded DNA and terminal deoxynucleotidyl transferase-mediated dUTP-biotin nick end-labeling (TUNEL) methods. Jpn J Cancer Res 90: 188–193.

Whelan HT, Smits RL Jr, Buchman EV, Whelan NT, Turner SG, Margolis DA, Cevenini V, Stinson H, Ignatius R, Martin T, Cwiklinski J, Philippi AF, Graf WR, Hodgson B, Gould L, Kane M, Chen G, Caviness J (2001) Effect of NASA light-emitting diode irradiation on wound healing. J Clin Laser Med Surg 19:305–314.

Whelan HT, Buchmann EV, Dhokalia A, Kane MP, Whelan NT, Wong-Riley MT, Eells JT, Gould LJ, Hammamieh R, Das R, Jett M (2003) Effect of NASA light-emitting diode irradiation on molecular changes for wound healing in diabetic mice. J Clin Laser Med Surg 21:67–74.

Wilden L, Karthein R (1998) Import of radiation phenomena of electrons and therapeutic low-level laser in regard to the mitochondrial energy transfer. J Clin Laser Med Surg 16:159–165.

Wong-Riley MTT, Bai XT, Buchmann E, Whelan HT (2001) Light-emitting diode treatment reverses the effect of TTX on cytochrome oxidase in neurons. Neuroreport 12:3033–3037.

Wong-Riley MTT, Whelan H, Dhokalia A, Das R, Hammamieh R, Liang HL, Eells J, Jett M (2002) cDNA microarray analysis of the visual cortex exposed to light-emitting diode treatment in monocularly enucleated rats. Soc Neurosci Abstr 131.20.

Wong-Riley MTT, Liang HL, Eells JT, Chance B, Henry MM, Buchmann E, Kane M, Whelan HT (2005) Photobiomodulation directly benefits primary neurons functionally inactivated by toxins: Role of cytochrome c oxidase. J Biol Chem 280:4761–4771.

Wu JM, Gorman A, Zhou XH, Sandra C, Chen EP (2002) Involvement of caspase-3 in photoreceptor cell apoptosis induced by in vivo blue light exposure. Invest Ophthalmol Vis Sci 43:3349–3354.

Yu W, Naim JO, McGowan M, Ippolito K, Lanzafame RJ (1997a) Photomodulation of oxidative metabolism and electron chain enzymes in rat liver mitochondria. Photochem Photobiol 66: 866–871.

Yu W, Naim JO, Lanzafame RJ (1997b) Effects of photostimulation on wound healing in diabetic mice. Lasers Surg Med 20:56–63.

Zhang C, Wong-Riley MTT (1999) Expression and regulation of NMDA receptor subunit R1 and neuronal nitric oxide synthase in cortical neuronal cultures: correlation with cytochrome oxidase. J Neurocytol 28:525–539.

Zhang J, Tan Z, Tran ND (2000) Chemical hypoxia-ischemia induces apoptosis in cerebromicrovascular endothelial cells. Brain Res 877:134–140.

Zhang HX, Li XQ, Tang T (2003) Characteristics of Bcl-2 and Bax expression in rat brain after experimental intracerebral hemorrhage and intervention of naoyian granule. Hunan Yi Ke Da Xue Xue Bao 28:229–232.

Zhao J, Schmid-Kotsas A, Gross HJ, Gruenert A, Bachem MG (2003) Sensitivity and specificity of different staining methods to monitor apoptosis induced by oxidative stress in adherent cells. Chin Med J 116:1923–1929.

Zhao L, Wu TW, Brinton RD (2004) Estrogen receptor subtypes alpha and beta contribute to neuroprotection and increased Bcl-2 expression in primary hippocampal neurons. Brain Res 1010:22–34.

(Accepted 20 December 2005)
(Available online 7 February 2006)